

# Fc gamma receptor IIb on target B cells promotes rituximab internalization and reduces clinical efficacy

Sean H. Lim,<sup>1</sup> Andrew T. Vaughan,<sup>1</sup> Margaret Ashton-Key,<sup>2</sup> Emily L. Williams,<sup>1</sup> Sandra V. Dixon,<sup>1</sup> H. T. Claude Chan,<sup>1</sup> Stephen A. Beers,<sup>1</sup> Ruth R. French,<sup>1</sup> Kerry L. Cox,<sup>1</sup> Andrew J. Davies,<sup>2</sup> Kathleen N. Potter,<sup>2</sup> C. Ian Mockridge,<sup>1</sup> David G. Oscier,<sup>3</sup> Peter W. M. Johnson,<sup>2</sup> \*Mark S. Cragg,<sup>1</sup> and \*Martin J. Glennie<sup>1</sup>

<sup>1</sup>Tenovus Research Laboratory, Cancer Sciences Division, Southampton University School of Medicine, General Hospital, Southampton, United Kingdom; <sup>2</sup>Cancer Research UK Experimental Cancer Medicine Centre, Cancer Sciences Division, Southampton University School of Medicine, General Hospital, Southampton, United Kingdom; and <sup>3</sup>Department of Haematology, Royal Bournemouth Hospital, Bournemouth, United Kingdom

**The anti-CD20 mAb rituximab is central to the treatment of B-cell malignancies, but resistance remains a significant problem. We recently reported that resistance could be explained, in part, by internalization of rituximab (type I anti-CD20) from the surface of certain B-cell malignancies, thus limiting engagement of natural effectors and increasing mAb consumption. Internalization of rituximab was most evident in chronic lymphocytic leukemia (CLL) and mantle cell lymphoma (MCL), but the extent of internalization was heteroge-**

**neous within each disease. Here, we show that the inhibitory FcγRIIb on target B cells promotes this process and is largely responsible for the observed heterogeneity across a range of B-cell malignancies. Internalization correlated strongly with FcγRIIb expression on normal and malignant B cells, and resulted in reduced macrophage phagocytosis of mAb-coated targets. Furthermore, transfection of FcγRIIb into FcγRIIb negative Ramos cells increased internalization of rituximab in a dose-dependent manner. Target-cell**

**FcγRIIb promoted rituximab internalization in a cis fashion and was independent of FcγRIIb on neighboring cells. It became phosphorylated and internalized along with CD20:anti-CD20 complexes before lysosomal degradation. In MCL patients, high FcγRIIb expression predicted less durable responses after rituximab-containing regimens. Therefore, target-cell FcγRIIb provides a potential biomarker of response to type I anti-CD20 mAb. (*Blood*. 2011;118(9):2530-2540)**

## Introduction

The anti-CD20 mAb rituximab has improved the overall survival of patients with follicular (FL) and diffuse large B-cell lymphoma (DLBCL).<sup>1-4</sup> However, in MCL, only modest responses are seen<sup>5</sup> and in CLL, fludarabine, cyclophosphamide and rituximab (FCR) therapy delivers improved responses but has yet to show a similar improvement in overall survival,<sup>6</sup> albeit the current follow-up is relatively short. Interestingly, those responses seen in CLL have often been achieved with high doses of rituximab,<sup>6</sup> suggesting that more mAb is needed to coat the targets or that it is consumed in some way. Even within rituximab-responsive lymphomas, a proportion of cases show resistance on first treatment with rituximab or eventually become resistant to rituximab-containing combination therapy (reviewed in Stolz et al<sup>7</sup>). The molecular basis of this resistance and the observed sensitivity of different lymphoma subtypes is unclear (reviewed in Lim et al<sup>8</sup>), but is highly relevant to improving outcomes.

In addition to understanding target resistance, many groups are working to deliver anti-CD20 mAb reagents with improved affinity and more potent engagement of cytotoxic effectors. Anti-CD20 mAb can be defined as type I (eg, rituximab, ofatumumab) or type II (eg, tositumumab, GA101), according to their ability to redistribute CD20 into lipid rafts in the plasma membrane and function in various effector assays.<sup>9-11</sup> It is still not clear what characteristics are required for the optimal reagent, but it is generally accepted that

FcγR interactions are crucial to the efficacy of anti-CD20 mAb.<sup>12-15</sup> In particular, FcγRIIIa on myeloid effectors appears critical in controlling Ab potency and in keeping with this, lymphoma patients bearing the higher affinity 158V allele in FcγRIIIa respond better to rituximab compared with those with the low affinity 158F allotype,<sup>16</sup> leading many investigators to focus on augmenting the interaction of mAb with FcγRIIIa, for example via defucosylation.<sup>17</sup>

Less attention has been given to the potential effects of the ITIM-containing inhibitory FcγR, FcγRIIb. FcγRIIb is a negative regulator of ITAM-containing receptors, such as the B-cell receptor (BCR) and the activatory FcγR.<sup>18</sup> Most hematopoietic cells coexpress inhibitory and activatory FcγR, and tumors are reported to be more sensitive to mAb immunotherapy in FcγRII<sup>-/-</sup> mice because of the removal of the inhibitory restraint of this receptor from myeloid effectors such as macrophages.<sup>12</sup> However, evidence of this inhibition in syngeneic tumor models and validation of the importance of FcγRIIb in the clinic is lacking.<sup>19,20</sup>

Early literature suggested that FcγRIIb is the predominant FcγR present on B cells,<sup>21</sup> although some later studies, primarily in human cell lines, also suggest the presence of FcγRIIa.<sup>22,23</sup> Our ongoing studies are in keeping with earlier literature, but require confirmation with FcγRIIb- or FcγRIIa-specific reagents. As a further complication, two alternatively spliced isoforms of FcγRIIb,

Submitted January 12, 2011; accepted July 3, 2011. Prepublished online as *Blood* First Edition paper, July 18, 2011; DOI 10.1182/blood-2011-01-330357.

\*M.S.C. and M.J.G. contributed equally to this article.

The online version of this article contains a data supplement.

The publication costs of this article were defrayed in part by page charge payment. Therefore, and solely to indicate this fact, this article is hereby marked "advertisement" in accordance with 18 USC section 1734.

© 2011 by The American Society of Hematology

Ib1 and Ib2 have been reported in humans and mice.<sup>21</sup> Mouse B cells only express Ib1<sup>24</sup> whereas both isoforms have been identified in human B-cell lines.<sup>22,23</sup> Ib1 and Ib2 isoforms appear to be functionally different, in that Ib2, but not Ib1 was reported to endocytose immune complexes.<sup>23-25</sup> This functional difference was observed in both mouse and human cells.

We recently demonstrated that CD20:anti-CD20 mAb complexes are internalized from the surface of B cells when treated with type I anti-CD20 mAb, but markedly less so with type II reagents.<sup>26</sup> Importantly, this difference in internalization appeared to explain much of the superior efficacy of type II mAb in deleting B cells in human CD20 transgenic mice. The rate of internalization of type I anti-CD20 mAb from the surface of different B cells (primary tumor versus cell-lines; CLL vs FL) differed markedly but the molecular explanation for this was unclear. We now show, using primary tumor material, that the Fc $\gamma$ RIIb expressed on target B cells engages rituximab on the same cell in a cis configuration and promotes internalization of CD20:mAb:Fc $\gamma$ RIIb tripartite complexes. Fc $\gamma$ RIIb expression was heterogeneous between different lymphoid tumors, and within each disease, and accounted for the differences in the rate and extent of anti-CD20 mAb internalization. Furthermore, we are able to correlate Fc $\gamma$ RIIb expression with clinical outcome in a small cohort of MCL patients treated with rituximab-containing regimens.

## Methods

### Cells

Human cell lines Raji and Ramos were obtained from ECACC and were maintained in antibiotic-free media (Roswell Park Memorial Institute [RPMI] medium; Invitrogen) supplemented with 10% FCS (Lonza) and glutamine and pyruvate (both Invitrogen). Rx3 Ramos cells lacking BCR expression were generated previously.<sup>27</sup> Ramos Fc $\gamma$ RIIb2 transfectants and control cells transfected with empty vectors (Fc $\gamma$ RIIb<sup>-</sup>) were previously described,<sup>27</sup> and were maintained in supplemented media as other human cell lines, with the addition of Geneticin (Invitrogen). Rx3 cells transfected with Fc $\gamma$ RIIb2 and empty vectors were produced and maintained in the same manner. Fc $\gamma$ RIIb surface expression was determined by flow cytometry using phycoerythrin (PE)-labeled AT10 (described in "Flow cytometry"). Populations of Ramos Fc $\gamma$ RIIb transfectants expressing low, medium or high levels of Fc $\gamma$ RIIb were sorted using a FACS Aria flow cytometer (BD Biosciences).

### Healthy blood donors

Normal human B cells were obtained from healthy volunteers with informed consent in accordance with the Declaration of Helsinki. Peripheral blood was taken in either EDTA or lithium heparin, lymphocytes separated using Lymphoprep (Axis-Shield) as per the manufacturer's protocol, and B cells isolated by negative selection with the human B-cell isolation kit II (Miltenyi Biotec). Similarly, monocytes were isolated using human monocyte isolation kit II (Miltenyi Biotec).

### Patient samples

Viable CLL/SLL, FL, DLBCL, and MCL samples were obtained with informed consent in accordance with the Declaration of Helsinki. Blood samples were collected in EDTA or lithium heparin with Lymphoprep and solid tissue was disaggregated through a sterile strainer and centrifuged. Cells were cryopreserved in RPMI supplemented with 50% human AB serum and 10% DMSO and stored in University of Southampton's Cancer Sciences Division Tumor Bank under Human Tissue Authority licensing. Ethical approval for the use of clinical samples was obtained by the Southampton University Hospitals NHS Trust from the Southampton and South West Hampshire Research Ethics Committee.

A series of paraffin-embedded tissue samples from MCL patients acquired in the last 10 years at Southampton General Hospital, United Kingdom were studied in accordance with a South West Hampshire Research Ethics Committee-approved protocol. The criteria for inclusion were patients treated with anti-CD20 mAb-containing therapy and availability of material for immunohistochemistry (IHC). Clinical information of the patients was collected by a clinician blinded to the IHC results. Demographic data are provided in supplemental Table 1 (available on the *Blood* Web site; see the Supplemental Materials link at the top of the online article). Progression-free survival (PFS) was measured from commencement of rituximab-containing therapy to either confirmed disease progression or death.

### Viability assay

Cells were assessed for viability by flow cytometry after staining with FITC-labeled annexin V and propidium iodide as detailed previously.<sup>9</sup>

### Antibodies and reagents

Rituximab was gifted by Southampton General Hospital oncology pharmacy. AT10 (produced in-house) is pan-specific for human Fc $\gamma$ RII, and binds to and blocks both Fc $\gamma$ RIIA and Fc $\gamma$ RIIb.<sup>28</sup> Tositumomab was gifted by Prof T. Illidge (University of Manchester, United Kingdom). Ofatumumab and GA101<sub>gly</sub> (glycosylated GA101 with unmodified Fc region) were produced in-house from patent published sequences. These mAb were produced in CHO or 293F cells and so may differ (eg, in their carbohydrate structures) from the mAb produced for clinical use. Alexa-488, anti-Alexa 488, Alexa-647 and streptavidin-linked Alexa-546 reagents were purchased from Invitrogen. Lysosomal marker, biotinylated LAMP-1 was purchased from eBioscience. Production of F(ab')<sub>2</sub> fragments has previously been described.<sup>29</sup> Fab' fragments were generated by incubation with 20mM 2-mercaptoethanol at 25°C, for 30 minutes, followed by addition of excess iodoacetamide. Western blotting antibodies used were anti-actin (AC74, Sigma-Aldrich), anti-tubulin and anti-phospho-Fc $\gamma$ RIIb (both CellSignaling Technology).

### Flow cytometry

Fluorochrome-labeled mAb were obtained from BD Biosciences or made in-house. mAb were conjugated with Alexa 488 (Invitrogen) as per the manufacturer's protocol. Flow cytometry has been described previously.<sup>30</sup> Samples were assessed on either a FACScan or FACSCalibur and data analyzed with CellQuest Pro Version 4.0.2 (all BD Biosciences) or FCS Express Version 3 Research Edition (DeNovo Software). B cells and macrophages were identified with allophycocyanin (APC)-labeled anti-human CD19 (in-house) and APC-labeled anti-CD16 (in-house), respectively, and Fc $\gamma$ RIIb expression determined using PE-labeled AT10 (in-house). To control for inter-experimental variation, Fc $\gamma$ RIIb expression was represented as the ratio of Fc $\gamma$ RIIb:isotype control Geo mean fluorescence intensity (MFI).

### Surface fluorescence quenching assay

The quenching assay was performed as detailed previously.<sup>26</sup> Briefly,  $2.4 \times 10^5$  cells per well were incubated with Alexa-488 labeled mAb at a final concentration of 5  $\mu$ g/mL. Samples were harvested after 1, 2, 6, and/or 24 hours, washed twice, resuspended and incubated at 4°C for 30 minutes with APC-labeled anti-CD19, with or without the quenching antibody, anti-Alexa-488 (Invitrogen). Samples were then washed once and analyzed on a flow cytometer. Only mAb that is remaining on the cell surface is accessible for quenching by anti-Alexa-488. Therefore, the results are represented as percent surface accessible anti-CD20, which is inversely proportional to the amount of mAb internalized.

To investigate the interaction of the Fc region of cell-bound anti-CD20 mAb with Fc $\gamma$ RIIb on adjacent cells, Ramos cells, which are Fc $\gamma$ RIIb<sup>-</sup>, were labeled with PKH26 (Sigma-Aldrich) as per the manufacturer's instructions. The PKH26-labeled cells were then cocultured with equal numbers ( $2.5 \times 10^5$  cells) of Ramos cells transfected with Fc $\gamma$ RIIb. Both cell types were cultured alone as controls. The quenching assay was then

performed as described above, and the internalization compared on the PKH26-labeled and -unlabeled populations. Further variations of this coculture assay are described in figure legends.

### Phagocytosis assay

As described earlier, monocytes were isolated from healthy human volunteers by negative selection. After a minimum of 2 hours adherence to plastic and washing, cells were cultured with RPMI supplemented with GP, autologous serum and antibiotics. To promote differentiation into macrophages, human monocyte colony stimulating factor (M-CSF, Peprotech) was added on alternate days at 50 ng/mL and the macrophages used after 7 days of culture. The phagocytosis assay has been previously described.<sup>26</sup>

### Western blotting

The protocol has been described previously.<sup>27</sup> Briefly,  $\sim 2 \times 10^6$  cells per well were incubated with mAb (5–10  $\mu$ g/mL). Samples were then separated by SDS-PAGE and proteins transferred immediately onto polyvinylidene membrane. Membranes were blocked with 5% wt/vol nonfat dried milk, incubated with the appropriately diluted primary antibodies, washed and then incubated with HRP-conjugated anti-rabbit or anti-mouse IgG (Sigma-Aldrich) and visualized by enhanced chemiluminescence (ECL, GE Healthcare or Pierce Biotechnology) and exposure to light-sensitive film (Hyperfilm ECL; GE Healthcare) or Biospectrum AC Imaging System (UVP).

### Light and confocal microscopy

To determine the intracellular trafficking of anti-CD20 mAb and Fc $\gamma$ RIIb, CLL cells were incubated with appropriate Alexa-488-labeled anti-CD20 mAb for various times as described in the figure legends and then harvested, washed and fixed with 2% paraformaldehyde. For detection of Fc $\gamma$ RIIb and LAMP-1, respectively, cells were then permeabilized with 0.3% saponin and incubated with Alexa-647-labeled AT10 F(ab')<sub>2</sub> (labeling performed with Alexa Fluor-647 labeling kit (Invitrogen) as per the manufacturer's protocol), and/or biotin conjugated anti-human LAMP-1. Cells were then washed, streptavidin-Alexa Fluor-547 added and followed by further washing. Cells were subsequently transferred onto slides and images captured using LAS-AF Version 2 software on a TCS-SP5 laser scanning confocal microscope (Leica Microsystems; 10 $\times$  eye piece, 100 $\times$  objective lens).

To determine cell proximity at different cell dilutions, cells were seeded at 1–20  $\times 10^5$ /mL, stimulated with various mAb for 2 or 6 hours and then their relative proximity assessed by light microscopy. Cells were viewed with an Olympus CKX21 inverted microscope (Olympus) using a 10 $\times$ /0.25 PH lens. Images were acquired using a CCL2 digital cooled camera (Olympus) and were processed with Cell B Version 2.6 (Olympus Soft Imaging Solutions) and Adobe Photoshop version CS2 software (Adobe).

To visualize phagocytosis, anti-CD20 mAb opsonized CFSE-labeled CLL cells were cocultured with macrophages in plastic chamber slides (Nunc) and inspected by confocal microscopy as above. To better delineate the macrophages, the cocultures were washed to remove nonadherent cells, fixed in acetone, dried and stained with May-Grünwald-Giemsa reagent before inspection with an Olympus CKX21 inverted microscope as above.

### Immunohistochemistry

Paraffin-embedded tissue blocks were cut into 4- $\mu$ m sections, mounted, dewaxed and immunostained with an anti-human Fc $\gamma$ RIIb antibody (clone EP888Y, Abcam). Immunohistochemical staining was performed using the fully automated Bond-Max (Leica Microsystems) immunostaining machine with Bond reagents as per the manufacturer's protocol. Briefly, the sections were first deparaffinized, and then pretreated by heat-induced epitope retrieval using the Bond ER2 protocol. The primary antibody was applied and incubated for 20 minutes followed by a peroxidase blocking step. Then, biotin-free, polymeric HRP-linked antibody conjugate detection system (Bond Polymer Refine Detection System) with 3,3'-diaminobenzidine as chromogen substrate was used. Slides were then counterstained with haematoxylin and mounted with Pertex (Histolab) using a Leica CV5330

machine. Ramos Fc $\gamma$ RIIa- and Fc $\gamma$ RIIb-transfected cells acted as negative and positive controls, respectively. MCL samples were considered Fc $\gamma$ RIIb positive membrane-staining was observed in at least 20% of tumor cells. Cytoplasmic staining without membrane-staining was considered to be Fc $\gamma$ RIIb negative. Immunostaining was interpreted by a histopathologist blinded to the clinical information.

### Statistical analysis

Statistical analysis was performed using GraphPad Prism Version 5 (GraphPad). All populations were assumed to be nonparametric and 2-tailed. Paired data were analyzed using the Wilcoxon's paired test and unpaired data using the Mann-Whitney test.

## Results

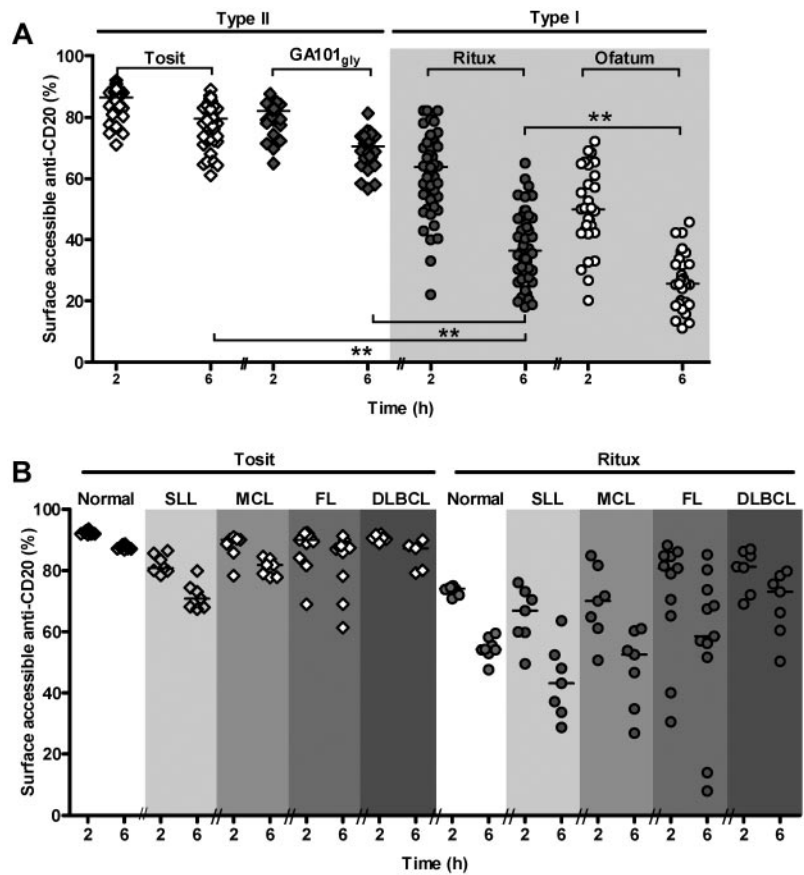
### Anti-CD20 mAb internalize heterogeneously in primary B-cell neoplasms

We previously observed heterogeneity in the rate and extent of internalization of rituximab in a small cohort of CLL samples.<sup>26</sup> Here, we validated these findings with a larger cohort of 48 CLL samples (Figure 1A). We compared the ability of type I (rituximab and ofatumumab) with type II (tositumomab and a nonglycomodified version of GA101 [GA101<sub>gly</sub>; type II])<sup>17</sup> to reduce the amount of surface accessible anti-CD20 mAb over 2, 6, and 24 hours (Figure 1A and data not shown). This internalization assay uses anti-Alexa-488 mAb to quench any Alexa-488-anti-CD20 mAb bound to the surface of the target cells. Alexa-488 labeled anti-CD20 mAb (anti-CD20-488) that has been internalized by the cells during culture cannot be quenched and remains fluorescent for detection by flow cytometry.<sup>31</sup> There was considerable heterogeneity but consistently treatment with type I mAb resulted in significantly more loss of CD20 from the cell surface than did type II mAb. At 6 hours, internalization of rituximab was near maximal (median 37% accessible at 6 hours) as it was for ofatumumab (median 26%; Figure 1A). In contrast, tositumomab and GA101<sub>gly</sub> showed less internalization, (median of 80% and 70% of bound mAb accessible at 6 hours, respectively).

Within the CLL cohort, we examined several biologic markers known to be important in the prognosis of CLL, including ZAP-70 expression,<sup>32,33</sup> CD38 expression<sup>34,35</sup> and IgVH gene mutation status.<sup>34,36,37</sup> No correlation was seen between any of these markers and internalization (supplemental Figure 1).

To explore the reason behind the heterogeneity in internalization of anti-CD20, we extended our previous cohort of primary samples to include 8 healthy volunteers, 7 small lymphocytic lymphoma (SLL), 7 MCL, 11 FL, and 7 DLBCL samples (Figure 1B). The difference in the ability of type I and II mAb to induce internalization persisted across all histologic subtypes. We also observed that rituximab on B cells from healthy volunteers internalized more uniformly than it did on malignant B cells, suggesting that factors associated with malignancy may contribute to the heterogeneity. The rate of rituximab internalization in CLL, SLL and MCL cells was similar, but generally slower in DLBCL and FL ( $P < .0001$  and  $.0027$ , respectively, Figure 1B compared with CLL from Figure 1A, Mann-Whitney test). Of note, in FL we observed 2 outliers that internalized rituximab very rapidly, leaving  $< 20\%$  detectable surface rituximab after 6 hours culture.

**Figure 1. Normal and malignant human B cells internalize type I anti-CD20 mAb.** (A) An in vitro surface fluorescence quenching assay as described in "Surface fluorescence quenching assay" was used to analyze primary CLL cells treated with Alexa-488-labeled mAb (Tosit-488, GA101gly-488, Ritux-488 or Ofatum-488, all 5  $\mu$ g/mL) for 2 or 6 hours ( $***P < .0001$ , Wilcoxon test). Internalization of anti-CD20 mAb is expressed as the percentage of anti-CD20 mAb detectable at the cell surface using secondary (quenching) anti-Alexa-488 mAb (surface accessible anti-CD20). Anti-CD20 mAb that has been internalized cannot be quenched by anti-Alexa-488 and so the cells remain fluorescent. (B) A variety of B-cell tumors and normal B cells from healthy volunteers were similarly examined after treatment with Tosit-488 or Ritux-488 (5  $\mu$ g/mL), and the extent of accessible mAb shown. Each point represents a sample from a different patient and medians are shown.



### Internalization of rituximab in B-cell lymphomas is an Fc-dependent process

We hypothesized that internalization might rely on the Fc region of the mAb and repeated the quenching assay with Alexa-488 labeled F(ab')<sub>2</sub> fragments of rituximab (Figure 2A). While the F(ab')<sub>2</sub> and IgG showed similar binding profiles (results not shown), the F(ab')<sub>2</sub> fragment internalized far less readily. These results indicate that an Fc-dependent mechanism may be involved in internalization and perhaps be responsible for at least part of the heterogeneity observed with the IgG. Since the assays were performed with highly enriched (>95% pure) B cells, the predominant Fc $\gamma$ R present in abundance should be the inhibitory Fc $\gamma$ RIIb.<sup>21</sup> Given the reported differences in endocytic capability between the IIB1 and IIB2 isoforms, we needed to confirm which isoform was expressed in primary human B cells. To ascertain this, RT-PCR was performed on purified normal B cells and CLL (supplemental Figure 2A). Both Fc $\gamma$ RIIb isoforms were detected, although interestingly CLL seem to express more IIB2 than IIB1 while the reverse was seen in normal B cells. All the samples selected were equally capable of internalizing rituximab, suggesting that at least in this context, both Fc $\gamma$ RIIb isoforms were functionally similar at promoting anti-CD20 mAb internalization.

Next, the pan anti-Fc $\gamma$ RII mAb, AT10 was used to block the interaction between the Fc domain of the anti-CD20 mAb and Fc $\gamma$ RIIb on B cells. As anticipated, internalization of rituximab was reduced (Figure 2B) and almost comparable with rituximab F(ab')<sub>2</sub> fragments (Figure 2A), confirming the involvement of Fc $\gamma$ RIIb.

These results indicated that Fc $\gamma$ RIIb on target B cells could play an important role in anti-CD20 mAb internalization, so we next

examined the expression of Fc $\gamma$ RIIb on the same clinical samples using AT10-PE. There was marked heterogeneity of Fc $\gamma$ RIIb expression within each group (Figure 2C) but with clear trends between diseases. Expression on CLL cells was relatively high, ranging from 20- to 300-fold over isotype control. DLBCL and the majority of FL displayed low Fc $\gamma$ RIIb expression. MCL and SLL expressed an intermediate albeit heterogeneous level of Fc $\gamma$ RIIb. It is of note that 2 cases of FL displayed very high Fc $\gamma$ RIIb expression, and strikingly, these were the same 2 'outliers' that internalized extremely rapidly (Figures 1B and 2C).

These findings were consistent with target-cell Fc $\gamma$ RIIb being an important participant in the internalization of rituximab from B-cell targets. When we compared the Fc $\gamma$ RIIb expression and rituximab internalization rates of all available samples (Figure 2D), Spearman correlation analysis revealed a strong relationship ( $r$  value  $-0.74$ , 95% confidence intervals:  $-0.83$  and  $-0.61$ , and  $P < .0001$ ). An inverse exponential curve could be drawn with DLBCL and most FL samples situated at the top of the curve, and MCL and CLL samples more broadly distributed.

### Fc $\gamma$ RIIb is a key participant in the internalization of rituximab

To corroborate the role of Fc $\gamma$ RIIb in this process, Ramos cells, which are Fc $\gamma$ RII<sup>-</sup> by flow cytometry (supplemental Figure 2B,E) were transfected with Fc $\gamma$ RIIb2, ie the predominant isoform observed in CLL cells (supplemental Figure 2A), and sorted into subclones expressing low, medium and high Fc $\gamma$ RIIb (Figure 2E). These cells, along with mock-transfected Fc $\gamma$ RIIb<sup>-</sup> Ramos cells were assessed in the quenching assay. The internalization of rituximab correlated with Fc $\gamma$ RIIb expression, with increasing

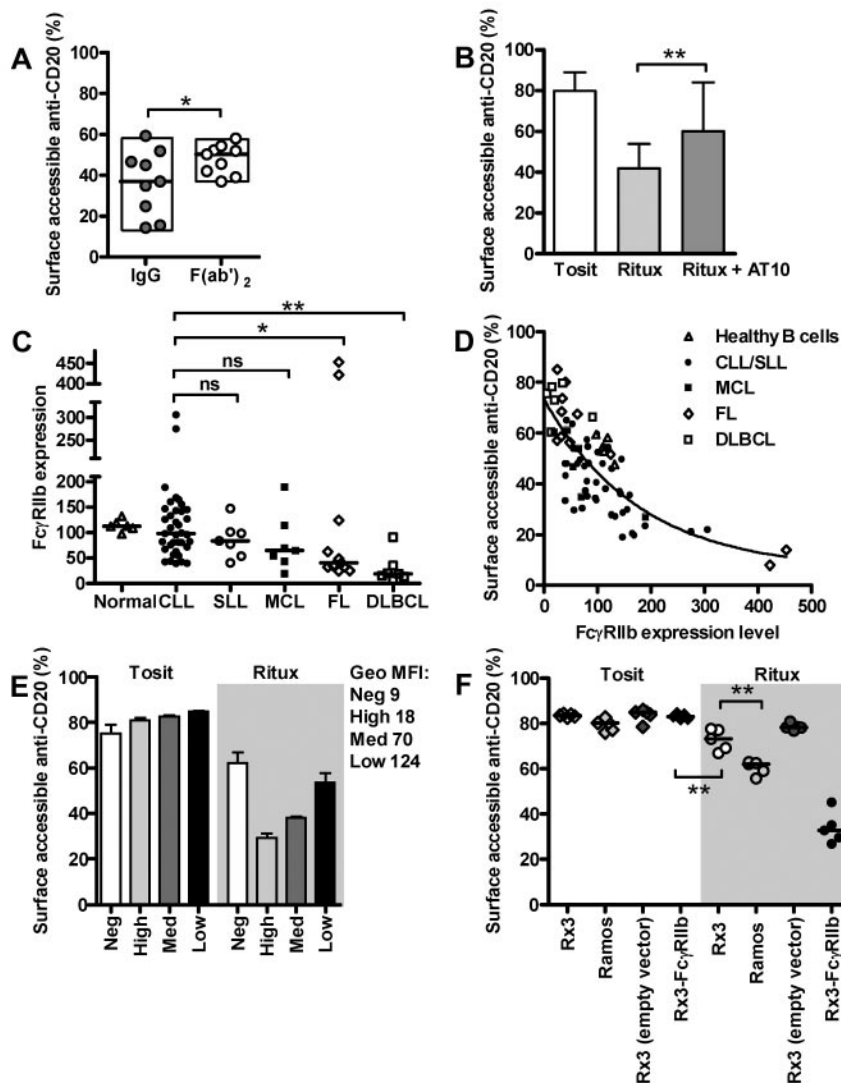


**Figure 2. Fc $\gamma$ RIIb participates in internalization of rituximab.** (A) The quenching assay in Figure 1A was repeated after treating CLL cells for 6 hours with Alexa-488-labeled F(ab')<sub>2</sub> or IgG molecules of rituximab (both 5  $\mu$ g/mL). \* $P$  < .05, Wilcoxon test. (B) The same assay was performed with Tosit-488 or Ritux-488 (both 5  $\mu$ g/mL)  $\pm$  addition of 10  $\mu$ g/mL blocking AT10 in CLL cells. Medians  $\pm$  ranges are shown (n = 6; \*\* $P$  < .001, Wilcoxon test). (C) Flow cytometric quantification of Fc $\gamma$ RIIb expression in healthy B cells and various B-cell tumors using AT10-PE. Medians are shown (\* $P$  < .05, \*\* $P$  < .001, Mann-Whitney test). (D) Fc $\gamma$ RIIb expression obtained in panel C correlated strongly with internalization of rituximab obtained in Figure 1 (after culture with Ritux-488 for 6 hours) across all lymphoma subtypes and normal B cells (Spearman  $r$  value = -.74; 95% confidence interval between -.83 and -.61;  $P$  < .0001). (E) Ramos cells transfected with Fc $\gamma$ RIIb were sorted by flow cytometry to express low, medium and high levels of Fc $\gamma$ RIIb and assessed in the quenching assay alongside mock-transfected cells after treatment with Tosit-488 or Ritux-488 (both 5  $\mu$ g/mL) for 6 hours. Data are represented as medians  $\pm$  ranges, n = 3. (F) The quenching assay was repeated with Tosit-488 or Ritux-488 (both 5  $\mu$ g/mL) on Rx3 cells (which lack BCR expression), Ramos cells, mock-transfected Rx3 cells and Fc $\gamma$ RIIb-transfected Rx3 cells after incubation for 6 hours. Median values are shown, \*\* $P$  = .0079, Mann-Whitney test.

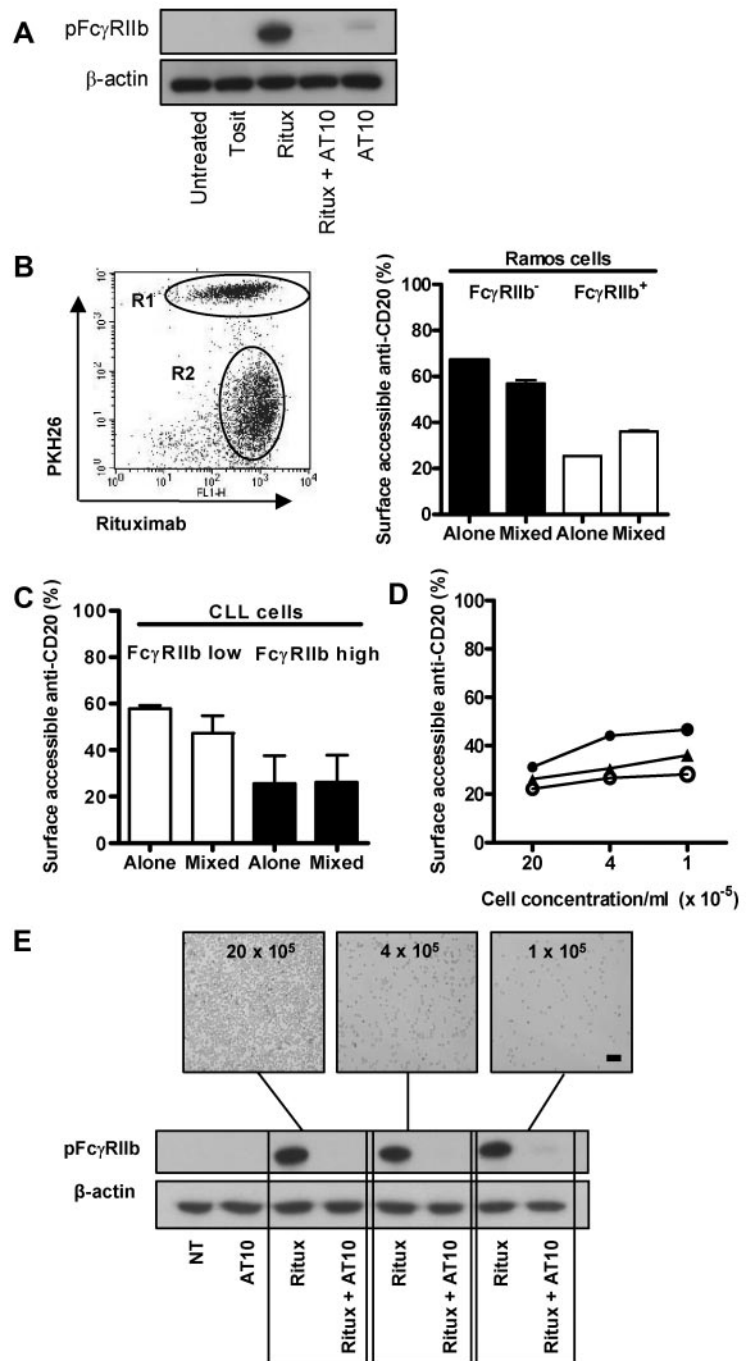
internalization in the order: Fc $\gamma$ RIIb<sup>-</sup> > Fc $\gamma$ RIIb<sup>+</sup> low > Fc $\gamma$ RIIb<sup>+</sup> medium > Fc $\gamma$ RIIb<sup>+</sup> high (Figure 2E).

As Fc $\gamma$ RIIb is a negative regulator of BCR activation on B cells and CD20 becomes physically associated with the BCR after binding of type I CD20 mAb,<sup>27,38</sup> we hypothesized that BCR expression or signaling activity could also influence internalization, particularly given the central role of the BCR in antigen uptake and internalization. To investigate the relative role of the BCR and Fc $\gamma$ RIIb in internalization of anti-CD20, BCR-deficient Ramos cells (Rx3) were transfected with Fc $\gamma$ RIIb, and compared with unmanipulated Ramos and mock-transfected Rx3 cells (Figure 2F). Rx3 cells lacking BCR expression internalize rituximab more slowly than Ramos cells, indicating a potential role for the BCR. However, this defect could be overcome by expressing Fc $\gamma$ RIIb (Fc $\gamma$ RIIb<sup>+</sup> Rx3 cells), indicating that BCR expression is not required for mAb internalization. Further evidence that the BCR is not a key determinant of internalization is derived from CLL cells, which characteristically express low levels of BCR,<sup>39</sup> yet displayed the highest levels of internalization. Furthermore, BCR expression levels on these cells were not predictive of rituximab internalization (supplemental Figure 1C).

#### Rituximab and Fc $\gamma$ RIIb crosslinking results in phosphorylation of Fc $\gamma$ RIIb and occurs predominantly in a cis fashion

We questioned whether the Fc $\gamma$ RIIb became activated during engagement by anti-CD20 mAb. Through immunoblotting, we observed phosphorylation of Fc $\gamma$ RIIb in both CLL and Raji lymphoma cells after rituximab treatment, but far less after tositumomab treatment, or when Fc $\gamma$ RIIb was blocked by the addition of AT10 (Figure 3A and supplemental Figure 3). This suggests that type I anti-CD20 mAb engages and then phosphorylates Fc $\gamma$ RIIb before internalization, since phosphorylation of Fc $\gamma$ RIIb occurs after only 0.5-2 hours of mAb treatment, when minimal internalization had occurred. However, it was not clear if coligation of CD20 and Fc $\gamma$ RIIb by type I anti-CD20 mAb occurred on the same (cis) or adjacent cells (trans). Elucidation of this is important because in vivo, other Fc $\gamma$ R-bearing cells could potentially compete for rituximab binding with Fc $\gamma$ RIIb. To address this question, we cocultured PKH26-labeled (Fc $\gamma$ RIIb<sup>-</sup>) Ramos cells with Fc $\gamma$ RIIb-high Ramos transfectants (Figure 3B). In the coculture, the level of internalization in the Fc $\gamma$ RIIb<sup>-</sup> cells was only slightly increased, and did not reach the level seen in the Fc $\gamma$ RIIb<sup>+</sup> cells (Figure 3B). We also cocultured a low Fc $\gamma$ RIIb-expressing PKH26 labeled-CLL sample with unlabeled cells from

**Figure 3. Rituximab binds CD20 and Fc $\gamma$ RIIb in a cis fashion and activates Fc $\gamma$ RIIb.** (A) Raji cells were stimulated with tositumomab, rituximab  $\pm$  AT10, or AT10 alone (all 10  $\mu$ g/mL) for 2 hours and assessed for phosphorylated Fc $\gamma$ RIIb by Western blotting. (B) PKH26-labeled Ramos cells (Fc $\gamma$ RIIb $^-$ , R1) were mixed 1:1 with sorted, high Fc $\gamma$ RIIb-expressing Ramos transfectants as described in "Surface fluorescence quenching assay" (R2, left). Fc $\gamma$ RIIb $^+$  and Fc $\gamma$ RIIb $^-$  cells were cultured alone, or mixed, and treated with 5  $\mu$ g/mL Ritux-488 for 6 hours (right) and assessed in the quenching assay. Data are represented as medians  $\pm$  ranges (n = 3). (C) As before, a low Fc $\gamma$ RIIb-expressing CLL sample was PKH26-labeled, mixed 1:1 with a high Fc $\gamma$ RIIb-expressing CLL sample and assessed in the quenching assay after treatment with 5  $\mu$ g/mL Ritux-488 for 6 hours. Data are represented as medians  $\pm$  ranges (n = 3). (D) CLL cells were cultured with Ritux-488 at various densities shown and the quenching assay performed after treatment with 5  $\mu$ g/mL Ritux-488 for 6 hours as before. (E) Raji cells were cultured at decreasing densities and assessed by Western blotting for phosphorylated Fc $\gamma$ RIIb. Representative images from these experiments demonstrate differences in cell proximity. Cells in were viewed while in culture using an Olympus CKX21 inverted microscope with a 10 $\times$ /0.25 PH lens and 10 $\times$  magnification was used. Bar represents 100  $\mu$ m.



3 different cases of CLL expressing high levels of Fc $\gamma$ RIIb (Figure 3C). In these mixed populations the internalization of rituximab by the Fc $\gamma$ RIIb-low CLL cells did not approach that seen with the Fc $\gamma$ RIIb-high CLL cells. Thus, rituximab internalization was a cell-intrinsic property which was not influenced by Fc $\gamma$ RIIb on neighboring cells. In an additional experiment of this type, Fc $\gamma$ RIIb-expressing CLL cells were cultured at decreasing concentrations to reduce the potential for cell:cell interaction. Reducing the cell density in this way made little difference to their ability to internalize rituximab (Figure 3D), consistent with there being little requirement for trans interaction between mAb and Fc $\gamma$ RIIb on adjacent cells. Finally, these observations were confirmed with the Fc $\gamma$ RIIb $^+$  human B-cell lymphoma line, Raji, which, like CLL, showed Fc $\gamma$ RIIb phosphorylation when

treated with rituximab but not tositumomab (Figure 3A). Light microscopy demonstrated that the likelihood of intercellular (trans) interaction was much less when cells were cultured at 1  $\times$  10 $^5$  compared with 2  $\times$  10 $^6$  cells/mL. Despite this, there was no marked difference in the levels of phosphorylated Fc $\gamma$ RIIb at different cell densities (Figure 3E). Altogether these experiments support the belief that internalization of rituximab by target-cell Fc $\gamma$ RIIb predominantly occurs in a cis fashion.

**Fc $\gamma$ RIIb is endocytosed with rituximab into lysosomes**

Given the cis mechanism of action and knowledge that rituximab becomes internalized, we postulated that Fc $\gamma$ RIIb is also internalized from the B-cell surface. First, we investigated whether binding

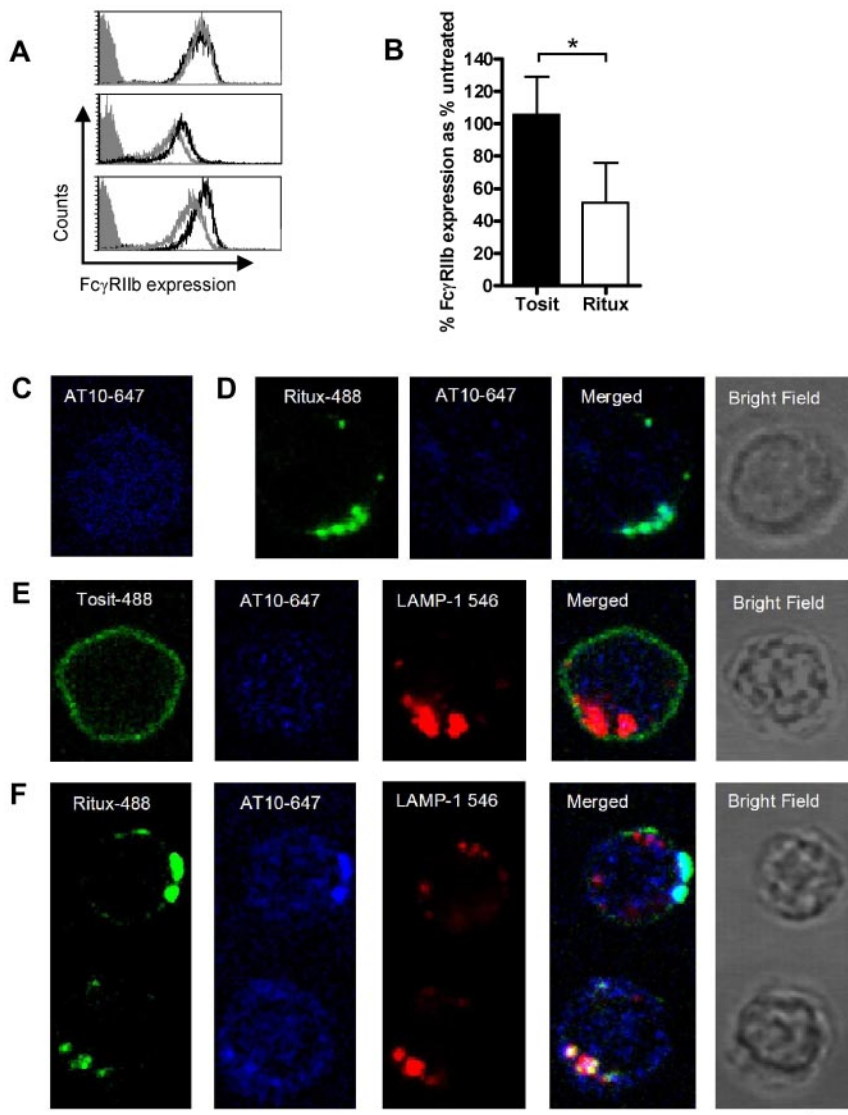


**Figure 4. Rituximab and Fc $\gamma$ RIIb internalize together into lysosomes.** (A) CLL cells were untreated, or treated with rituximab for 30 minutes on ice, washed, and then stained with AT10-PE and analyzed by flow cytometry. Representative histograms from 3 patients are shown. (gray-filled: isotype control; black line: AT10 expression of untreated cells; gray line: AT10 expression of rituximab treated cells). (B) CLL cells were incubated with Tosit-488 or Ritux-488 (5  $\mu$ g/mL) for 2 hours and then Fc $\gamma$ RIIb expression detected using AT10-PE. Data are represented as medians  $\pm$  ranges (n = 6; \*P = .0313, Wilcoxon test). (C) Untreated CLL cells were cultured for 6 hours, then fixed and permeabilized with saponin. Intracellular Fc $\gamma$ RIIb was detected using AT10-647 (blue) and the cells analyzed by confocal microscopy. (D,E) Cells from the same CLL sample as in panel C were cultured with Ritux-488 (green) for 30 minutes (D) or Tosit-488 (green; E) for 6 hours and then treated as described in panel C for detection of intracellular Fc $\gamma$ RIIb with AT10-647. In addition the Tosit-488 cultured cells were also so stained with biotinylated LAMP-1 and streptavidin-546 (red) to detect lysosomes. (F) CLL cells were treated with Ritux-488 for 6 hours and assessed as in panel E. 2 representative cells are shown. The top cell shows unambiguous colocalization between Ritux-488 and Fc $\gamma$ RIIb, but no colocalization with LAMP-1. The bottom cell shows colocalization of all 3 mAb. In each case the bright field image is shown from the same cell. A Leica TCS-SP5 laser scanning confocal microscope with 10 $\times$  eye piece, 100 $\times$  objective oil immersion lens was used in each case. Bar represents 5  $\mu$ m.

of the Fc region of anti-CD20 mAb blocked subsequent binding of AT10 to Fc $\gamma$ RIIb. To do so, CLL cells were first treated with rituximab, or left untreated, for 30 minutes on ice to prevent internalization. The cells were then washed, before assessing Fc $\gamma$ RIIb expression with AT10-PE. Pre-treating cells with rituximab made little difference to the binding of AT10-PE (Figure 4A), suggesting that the relatively weak interaction between the rituximab Fc and Fc $\gamma$ RIIb at the cell surface is unable to block the high affinity binding of AT10 to Fc $\gamma$ RIIb. This is consistent with AT10 binding and blocking the ability of Fc $\gamma$ RIIb to promote rituximab internalization (Figure 2B). Having established that AT10 would detect Fc $\gamma$ RIIb in the presence of rituximab, we next assessed the surface expression of Fc $\gamma$ RIIb on 6 different CLL samples and found that it declined within 2 hours of incubation with rituximab but not tositumomab (Figure 4B). These findings are consistent with Fc $\gamma$ RIIb being internalized along with CD20 and rituximab (but not tositumomab) as part of a tripartite complex.

To identify whether the components of the complex trafficked to similar intracellular compartments, CLL cells were treated with either Tosit-488 or Ritux-488 for 30 minutes or 6 hours to allow detection of internalized anti-CD20. The treated cells were then

permeabilized and intracellular Fc $\gamma$ RIIb and lysosomes detected using Alexa 647-labeled AT10 (AT10-647) and streptavidin-linked Alexa-546/biotinylated LAMP-1 mAb, for Fc $\gamma$ RIIb and lysosome detection, respectively. Before anti-CD20 mAb treatment, Fc $\gamma$ RIIb staining was diffuse and nonlocalized (Figure 4C). However, after 30 minutes treatment with Ritux-488, Fc $\gamma$ RIIb staining was visibly different, showing punctate staining that colocalized with Ritux-488 (Figure 4D). In contrast, even after 6 hours treatment with Tosit-488, the pattern of Fc $\gamma$ RIIb staining (Figure 4E) was comparable with untreated cells (Figure 4C). Furthermore, at 6 hours, a distinct difference in staining between Ritux-488 and Tosit-488 was observed, with Tosit-488 remaining predominantly on the surface (Figure 4E) and Ritux-488 showing punctate staining (Figure 4F), consistent with our previous observations.<sup>26</sup> In Tosit-488-treated cells, no colocalization was seen either with Fc $\gamma$ RIIb or lysosomes (Figure 4E) whereas Ritux-488 colocalized with AT10-647 in 58% of cells (Figure 4F). Colocalization of Ritux-488, LAMP-1 and AT10-647 was observed in 33% of cells. Presumably, this lower degree of colocalization observed between all 3 fluorochromes reflects the fact that Ritux-488 and Fc $\gamma$ RIIb internalize together and are likely to occupy compartments other

than endosomes and lysosomes in view of the known pathways of intracellular trafficking of synthetic macromolecules.<sup>40</sup> Whether this translates to reduced lysosomal degradation or not, is not clear at this stage.

### Fc $\gamma$ RIIb inhibition enhances phagocytosis of rituximab-treated CLL cells

We previously demonstrated that internalization of anti-CD20 mAb was associated with reduced phagocytosis of mouse B cells.<sup>26</sup> To ascertain that internalization was equally relevant in human cells, a phagocytosis assay was performed using CFSE-labeled CLL cells. The cells were treated with anti-CD20 mAb (GA101<sub>gly</sub> or rituximab) for 15 minutes, or 6 hours to allow internalization. Excess mAb was removed and then cells were ‘fed’ to human macrophages. Phagocytosis of CLL cells could be visualized by light microscopy (Figure 5A). For more objective assessment, macrophages were identified using anti-CD16-APC and analyzed by flow cytometry. Double-positive (CFSE<sup>+</sup> CD16<sup>+</sup>) cells represent macrophages that have phagocytosed CLL cells, or have the CLL cells rosetted on their surface (Figure 5B top panels). Treatment of CLL cells with rituximab for 6 hours compared with 15 minutes resulted in a ~30% reduction in phagocytosis, whereas treatment with GA101<sub>gly</sub> showed only a ~10% reduction (Figure 5B bottom panel). This difference in phagocytic activity between the 2 types of anti-CD20 mAb was significant, but may appear modest compared with the marked difference in the ability of these mAb to undergo internalization (Figure 1). However, the quenching assay used earlier is far more sensitive at detecting and quantifying changes in surface mAb levels than the phagocytosis assay. Importantly, maximal phagocytosis for rituximab was restored through blocking of Fc $\gamma$ RIIb on CLL cells using AT10 F(ab')<sub>2</sub> fragments (Figure 5C).

### Fc $\gamma$ RIIb levels predict clinical outcome in rituximab-treated MCL patients

As proof-of-principle of our *in vitro* findings, we retrospectively examined the Fc $\gamma$ RIIb expression of a small cohort of MCL patients who had received rituximab-based therapies. Diagnostic paraffin-embedded tissue was stained by IHC using an Fc $\gamma$ RIIb-specific mAb (supplemental Figure 2). Samples were considered Fc $\gamma$ RIIb<sup>+</sup> when >20% of tumor cells showed membrane staining, although in practice overwhelming membrane staining was usually observed. Using a set of lymphoma samples for which viable cells were also available, we were able to confirm that IHC results corresponded with Fc $\gamma$ RIIb expression levels obtained by flow cytometry (Figure 6A inset values). Using a small cohort of 16 MCL patients, we demonstrate that patients with Fc $\gamma$ RIIb<sup>-</sup> lymphoma had significantly better median progression-free survival than those with Fc $\gamma$ RIIb<sup>+</sup> cells (median 852 and 189 days, respectively,  $P < .05$ ; Figure 6B left panel). The groups had comparable demographic data and MCL international prognostic index scores,<sup>41</sup> (supplemental Table 1), but there was heterogeneity in the chemotherapy types used. To address this, we examined the results in those patients treated with either single-agent rituximab or FCR for initial therapy, and similar results were observed but statistical significance was not achieved likely because of the limited number of cases examined (Figure 6B right panel; median survival 850 and 125 for Fc $\gamma$ RIIb<sup>-</sup> and Fc $\gamma$ RIIb<sup>+</sup> groups, respectively).

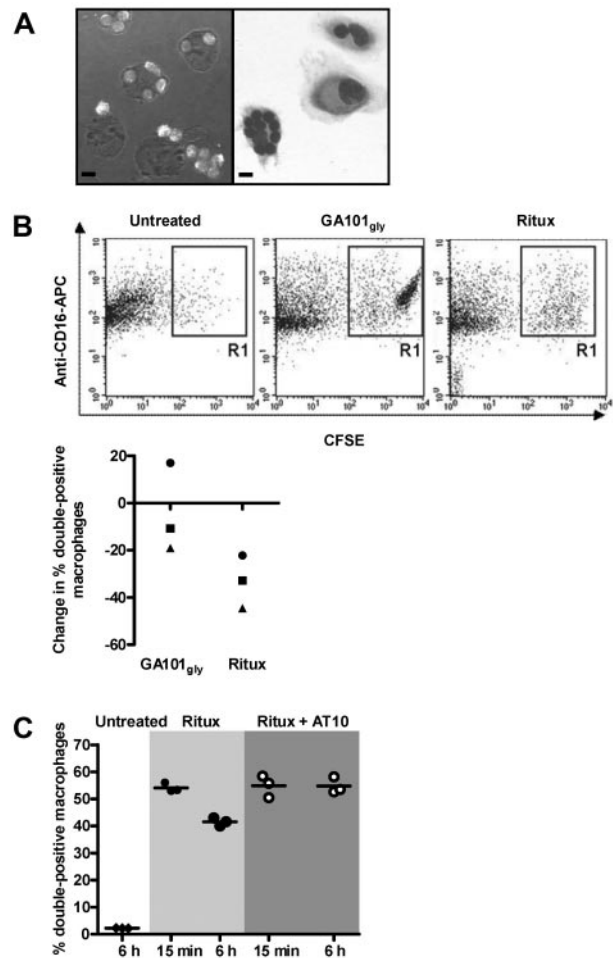


**Figure 5. Fc $\gamma$ RIIb inhibition promotes phagocytosis of rituximab-treated CLL cells.** (A) Phagocytosis assays: CFSE-labeled CLL cells were treated with GA101<sub>gly</sub> for 6 hours and then added to normal human macrophages for phagocytosis. Representative images are shown by confocal microscopy (left) and after May-Grünwald-Giemsa staining by bright field microscopy (right). Bar represents 10  $\mu$ m. A Leica TCS-SP5 laser scanning confocal microscope (10 $\times$  eye piece, 40 $\times$  objective oil immersion lens) and Olympus CKX21 inverted microscope with 10 $\times$ /0.25PH lens with 40 $\times$  objective oil immersion lens was used, respectively. (B) The assay in panel A was repeated but CFSE-labeled CLL cells were treated with either GA101<sub>gly</sub> or rituximab for 15 minutes or 6 hours before adding to the macrophages. Anti-CD16-APC was used to identify the macrophages, and results were analyzed by flow cytometry. Representative dot plots are shown for untreated and treated cells (top panels). Double-positive cells include both macrophages that have phagocytosed CFSE-labeled CLL cells, and also macrophages that have them rosetted on their surface. However, visual analysis of confocal images as in panel A suggests that >90% of the CFSE-labeled CLL cells have been phagocytosed. The graph (bottom panel) shows the reduction in the % double positive cells between 15 minutes and 6 hours. Each point shows the mean of triplicate samples, and 3 different CLL patients are shown. Different symbols are used to identify samples from the same patients. (C) As in panel B, but CLL cells were treated with rituximab only, or in combination with AT10 F(ab')<sub>2</sub> for 15 minutes or 6 hours and phagocytosis measured. Triplicate samples are shown; the experiment has been repeated twice.

## Discussion

Our previous work showed that internalization of type I anti-CD20 mAb has 2 important consequences for mAb immunotherapy; it reduces the amount of IgG at the cell surface available to recruit effectors and it consumes mAb.<sup>26</sup> We now demonstrate a key molecular component of this internalization and demonstrate that a mechanism of tumor resistance by which Fc $\gamma$ RIIb on the primary B cells promotes internalization. When primary lymphoma cells were cultured with type I, but not with type II anti-CD20 mAb,



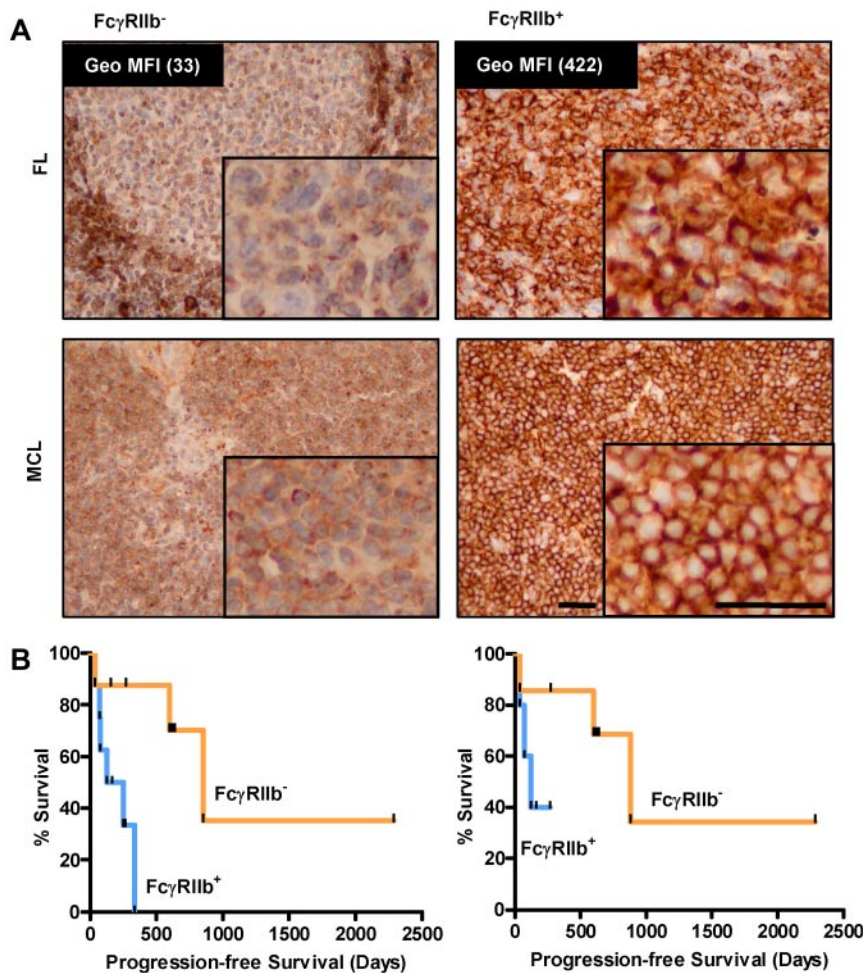


**Figure 6. Fc $\gamma$ RIIb levels predict progression-free survival in MCL patients treated with rituximab regimens.** (A) Immunohistochemistry for Fc $\gamma$ RIIb in FL (top panel, flow cytometric quantification of Fc $\gamma$ RIIb expression of corresponding viable cells shown and MCL bottom panel) samples. Representative examples of negative (left) and positive membranous (right) staining are shown. The top left panel demonstrates Fc $\gamma$ RIIb staining in the normal mantle region, which serves as an internal positive control for the staining. (B) Progression-free survival of 16 MCL patients treated with rituximab-containing regimens classified on the basis of positive or negative Fc $\gamma$ RIIb expression by immunohistochemistry (left,  $n = 8$  per group,  $P < .05$ , log-rank test), and 12 MCL patients treated with frontline FCR or rituximab alone (right,  $n = 6$  per group,  $P$  value not significant, log-rank test).

significant but heterogeneous internalization was observed. Furthermore, cases of MCL and CLL typically undergoing internalization more rapidly and extensively than FL and DLBCL. This is interesting because rituximab is of most proven benefit in DLBCL and FL where, in combination with chemotherapy, it is established first-line therapy. By contrast, relatively less benefit is seen in CLL<sup>6,42</sup> and MCL.<sup>5</sup> As B-cell malignancies that express higher Fc $\gamma$ RIIb (CLL and MCL) are more likely to internalize rituximab (and other type I anti-CD20 mAb), we now suggest that this could explain some of the clinical heterogeneity observed in the different lymphoma subtypes in response to rituximab. In the case of CLL, the lack of response has often been attributed to weak expression of CD20 but internalization is an equally plausible explanation. Furthermore, this explanation is in keeping with the extensive consumption of rituximab often reported in CLL patients and the need to deliver higher doses than those required in FL or DLBCL.<sup>6,42</sup>

There is some contention that B cells not only express Fc $\gamma$ RIIb, but also Fc $\gamma$ RIIa. Most of these investigations were carried out using cell lines in which low levels of Fc $\gamma$ RIIa were reported,<sup>22</sup> and differ from studies with primary human cells which found only Fc $\gamma$ RIIb.<sup>21</sup> Our own ongoing studies suggest that only Fc $\gamma$ RIIb is present on the surface of primary human B cells (S.H.L., unpublished observations, November 2010). Both Iib1 and Iib2 Fc $\gamma$ RIIb isoforms have been documented in human B cells, unlike mouse B cells, where only Iib1 is shown.<sup>22,24</sup> It is suggested that the 2 isoforms differ in terms of their ability to internalize immune complexes,<sup>24</sup> but we found no evidence for such a functional

distinction since both normal B cells and CLL cells, which differ in their expression of the 2 isoforms, had a similar ability in mediating endocytosis of rituximab. Studies are underway to examine the Iib1:Iib2 isoform expression pattern in other primary malignant B-cell subtypes and to address specifically the role of the different Fc $\gamma$ RIIb isoforms in these cells.

Our investigations suggest that rituximab can cocrosslink CD20 and Fc $\gamma$ RIIb predominantly on the same target B cell, resulting in phosphorylation of Fc $\gamma$ RIIb, and internalization of CD20:rituximab:Fc $\gamma$ RIIb complexes into lysosomes for degradation. The strong correlation between the internalization of rituximab and Fc $\gamma$ RIIb expression on B cells suggests that Fc $\gamma$ RIIb is a key participant. However, when cells were cultured with either F(ab')<sub>2</sub> or a combination of a type I anti-CD20 mAb and a blocking anti-Fc $\gamma$ RII mAb, the reduced level of internalization was still more than that induced by type II anti-CD20 mAb. This suggests that other factors participate in the internalization of anti-CD20 and that these predispose type I reagents to internalize. Our findings indicate that BCR function is not a major factor. Alternatively, differences in lipid raft translocation or membrane fluidity could influence internalization, and this is currently under investigation. It is similarly unclear, why type II anti-CD20 mAb tend not to internalize and do not engage and activate Fc $\gamma$ RIIb, but this may relate to differences in orientation of type II mAb after binding.<sup>43</sup>

Other groups have studied the association between Fc $\gamma$ RIIb expression on B cells and response to rituximab in B-cell lymphoma. Camilleri-Broet et al analyzed Fc $\gamma$ RIIb expression in DLBCL patients treated with first-line R-CHOP.<sup>44</sup> No correlation

was found between FcγRIIb expression on tumor cells and survival after R-CHOP, which appears to contradict our current findings. However, the level of expression in positive cases is unknown and this aspect may be of particular importance as our flow cytometry data indicate that the same B-cell malignancies can have a broad spectrum of FcγRIIb expression level. When the matched paraffin-embedded samples are stained by IHC, the spectrum of expression differences was not immediately apparent and could only be interpreted as positive or negative, as described in the methodology. Furthermore, in our hands, IHC was very sensitive and FcγRIIb<sup>+</sup> cases corresponded with Geo MFI expression levels as low as 40 (data not shown). This level may be too low to stratify with survival in a disease such as DLBCL where the FcγRIIb expression range is far narrower than in MCL. We predict that flow cytometry may be more informative for these diseases.

As far as we are aware, ours is the first study to present suggestive clinical evidence of the association between FcγRIIb expression and response to rituximab treatment in a B-cell neoplasm. Because of the limited number of MCL cases, the clinical findings require validation with a larger sample but in this context, the clinical data serves to complement the experimental findings. Ongoing efforts are being made to study the role of FcγRIIb as a biomarker of response in CLL and FL.

In summary, our work has 2 major implications. First, response to anti-CD20 mAb therapy may be optimized using type II anti-CD20 mAbs such as GA101, which circumvent the limitations of internalization, regardless of FcγRIIb expression. Alternatively, concurrent administration of an FcγRIIb inhibitor with rituximab may potentiate its therapeutic efficacy in cases of high FcγRIIb expression. Finally, this work uncovers a previously unrecognized means by which FcγRIIb may reduce the efficacy of mAb immunotherapy. This gives further impetus to investigate the association between FcγRIIb expression and response to mAb immunotherapy in B-cell neoplasms.

## References

- Feugier P, Van Hoof A, Sebban C, et al. Long-term results of the R-CHOP study in the treatment of elderly patients with diffuse large B-cell lymphoma: a study by the Groupe d'Etude des Lymphomes de l'Adulte. *J Clin Oncol*. 2005; 23(18):4117-4126.
- Sehn LH, Donaldson J, Chhanabhai M, et al. Introduction of combined CHOP plus rituximab therapy dramatically improved outcome of diffuse large B-cell lymphoma in British Columbia. *J Clin Oncol*. 2005;23(22):5027-5033.
- Marcus R, Imrie K, Belch A, et al. CVP chemotherapy plus rituximab compared with CVP as first-line treatment for advanced follicular lymphoma. *Blood*. 2005;105(4):1417-1423.
- Marcus R, Imrie K, Solal-Celigny P, et al. Phase III study of R-CVP compared with cyclophosphamide, vincristine, and prednisone alone in patients with previously untreated advanced follicular lymphoma. *J Clin Oncol*. 2008;26(28):4579-4586.
- Lenz G, Dreyling M, Hoster E, et al. Immunotherapy with rituximab and cyclophosphamide, doxorubicin, vincristine, and prednisone significantly improves response and time to treatment failure, but not long-term outcome in patients with previously untreated mantle cell lymphoma: results of a prospective randomized trial of the German Low Grade Lymphoma Study Group (GLSG). *J Clin Oncol*. 2005;23(9):1984-1992.
- Hallek M, Fischer K, Fingerle-Rowson G, et al. Addition of rituximab to fludarabine and cyclophosphamide in patients with chronic lymphocytic leukaemia: a randomised, open-label, phase 3 trial. *Lancet*. 2010;376(9747):1164-1174.
- Stolz C, Schuler M. Molecular mechanisms of resistance to Rituximab and pharmacologic strategies for its circumvention. *Leuk Lymphoma*. 2009;50(6):873-885.
- Lim SH, Beers SA, French RR, Johnson PW, Glennie MJ, Cragg MS. Anti-CD20 monoclonal antibodies: historical and future perspectives. *Haematologica*. 2010;95(1):135-143.
- Chan HT, Hughes D, French RR, et al. CD20-induced lymphoma cell death is independent of both caspases and its redistribution into triton X-100 insoluble membrane rafts. *Cancer Res*. 2003;63(17):5480-5489.
- Cragg MS, Glennie MJ. Antibody specificity controls in vivo effector mechanisms of anti-CD20 reagents. *Blood*. 2004;103(7):2738-2743.
- Ivanov A, Beers SA, Walshe CA, et al. Monoclonal antibodies directed to CD20 and HLA-DR can elicit homotypic adhesion followed by lysosome-mediated cell death in human lymphoma and leukemia cells. *J Clin Invest*. 2009;119(8):2143-2159.
- Clynes RA, Towers TL, Presta LG, Ravetch JV. Inhibitory Fc receptors modulate in vivo cytotoxicity against tumor targets. *Nat Med*. 2000;6(4):443-446.
- Uchida J, Hamaguchi Y, Oliver JA, et al. The innate mononuclear phagocyte network depletes B lymphocytes through Fc receptor-dependent mechanisms during anti-CD20 antibody immunotherapy. *J Exp Med*. 2004;199(12):1659-1669.
- Nimmerjahn F, Ravetch JV. Antibodies, Fc receptors and cancer. *Curr Opin Immunol*. 2007;19(2):239-245.
- Beers SA, Chan CH, James S, et al. Type II (tositumomab) anti-CD20 monoclonal antibody outperforms type I (rituximab-like) reagents in B-cell depletion regardless of complement activation. *Blood*. 2008;112(10):4170-4177.
- Weng WK, Levy R. Two immunoglobulin G fragment C receptor polymorphisms independently predict response to rituximab in patients with follicular lymphoma. *J Clin Oncol*. 2003;21(21):3940-3947.
- Mossner E, Brunker P, Moser S, et al. Increasing the efficacy of CD20 antibody therapy through the engineering of a new type II anti-CD20 antibody with enhanced direct- and immune effector cell-mediated B-cell cytotoxicity. *Blood*. 2010;115(22):4393-4402.
- Nimmerjahn F, Ravetch JV. Fcγ receptors as regulators of immune responses. *Nat Rev Immunol*. 2008;8(1):34-47.
- Camilleri-Broet S, Mounier N, Delmer A, et al. FcγRIIb expression in diffuse large B-cell lymphomas does not alter the response to CHOP + rituximab (R-CHOP). *Leukemia*. 2004; 18(12):2038-2040.
- Weng WK, Levy R. Genetic polymorphism of the inhibitory IgG Fc receptor FcγRIIb is not associated with clinical outcome in patients with follicular lymphoma treated with rituximab. *Leuk Lymphoma*. 2009;50(5):723-727.
- Brooks DG, Qiu WQ, Luster AD, Ravetch JV.

## Acknowledgments

The authors are grateful to I. Wheatley and A. Tilbury for provision and assistance with clinical material, S. Barton for statistical advice and N. George for technical assistance with immunohistochemistry.

Funding was provided by a Medical Research Council fellowship to S.H.L., Leukemia and Lymphoma Research grants 07 048 and 09 009, Cancer Research UK grants C328/A2738 and C328/A2737 and Tenovus, Cardiff.

S.H.L. dedicates this work to her father, Tee Seong Lim, in his personal battle against cancer.

## Authorship

Contribution: S.H.L. performed research, analyzed and interpreted data and wrote the manuscript; A.V., M.K., E.L.W., S.V.D., S.A.B., R.R.F., K.L.C., A.J.D., D.G.O., K.N.P. and C.I.M. performed research; C.H.T.C. contributed vital new reagents; P.W.M.J. analyzed and interpreted data; and M.J.G. and M.S.C. designed research, analyzed and interpreted data and wrote the manuscript.

Conflict-of-interest disclosure: P.W.M.J. has participated on the advisory boards for Roche, Genentech, and GSK and the data monitoring committee for Genmab. A.J.D. has also participated on the advisory boards for Roche and GSK. The remaining authors declare no competing financial interests.

Correspondence: Martin J. Glennie, Tenovus Research Laboratory, Mailpoint 88, Southampton General Hospital, Tremona Road, Southampton, SO16 6YD, United Kingdom; e-mail: mjg@soton.ac.uk.

- Structure and expression of human IgG FcRII(CD32). Functional heterogeneity is encoded by the alternatively spliced products of multiple genes. *J Exp Med*. 1989;170(4):1369-1385.
22. Cassel DL, Keller MA, Surrey S, et al. Differential expression of Fc gamma RIIA, Fc gamma RIIb and Fc gamma RIIC in hematopoietic cells: analysis of transcripts. *Mol Immunol*. 1993;30(5):451-460.
  23. Van Den Herik-Oudijk IE, Westerdaal NA, Henriquez NV, Capel PJ, Van De Winkel JG. Functional analysis of human Fc gamma RII (CD32) isoforms expressed in B lymphocytes. *J Immunol*. 1994;152(2):574-585.
  24. Miettinen HM, Rose JK, Mellman I. Fc receptor isoforms exhibit distinct abilities for coated pit localization as a result of cytoplasmic domain heterogeneity. *Cell*. 1989;58(2):317-327.
  25. Budde P, Bewarder N, Weinrich V, Schulzeck O, Frey J. Tyrosine-containing sequence motifs of the human immunoglobulin G receptors FcRIIb1 and FcRIIb2 essential for endocytosis and regulation of calcium flux in B cells. *J Biol Chem*. 1994;269(48):30636-30644.
  26. Beers SA, French RR, Chan HT, et al. Antigenic modulation limits the efficacy of anti-CD20 antibodies. *Blood*. 2010;115(25):5191-5201.
  27. Walshe CA, Beers SA, French RR, et al. Induction of cytosolic calcium flux by CD20 is dependent upon B Cell antigen receptor signaling. *J Biol Chem*. 2008;283(25):16971-16984.
  28. Greenman J, Tutt AL, George AJ, Pulford KA, Stevenson GT, Glennie MJ. Characterization of a new monoclonal anti-Fc gamma RII antibody, AT10, and its incorporation into a bispecific F(ab')<sub>2</sub> derivative for recruitment of cytotoxic effectors. *Mol Immunol*. 1991;28(11):1243-1254.
  29. Glennie MJ, McBride HM, Worth AT, Stevenson GT. Preparation and performance of bispecific F(ab')<sub>2</sub> antibody containing thioether-linked Fab' gamma fragments. *J Immunol*. 1987;139(7):2367-2375.
  30. Tutt AL, French RR, Illidge TM, et al. Monoclonal antibody therapy of B cell lymphoma: signaling activity on tumor cells appears more important than recruitment of effectors. *J Immunol*. 1998;161(6):3176-3185.
  31. Austin CD, De Maziere AM, Pisacane PI, et al. Endocytosis and sorting of ErbB2 and the site of action of cancer therapeutics trastuzumab and geldanamycin. *Mol Biol Cell*. 2004;15(12):5268-5282.
  32. Wiestner A, Rosenwald A, Barry TS, et al. ZAP-70 expression identifies a chronic lymphocytic leukemia subtype with unmutated immunoglobulin genes, inferior clinical outcome, and distinct gene expression profile. *Blood*. 2003;101(12):4944-4951.
  33. Crespo M, Bosch F, Villamor N, et al. ZAP-70 expression as a surrogate for immunoglobulin-variable-region mutations in chronic lymphocytic leukemia. *N Engl J Med*. 2003;348(18):1764-1775.
  34. Damle RN, Wasil T, Fais F, et al. Ig V gene mutation status and CD38 expression as novel prognostic indicators in chronic lymphocytic leukemia. *Blood*. 1999;94(6):1840-1847.
  35. Ibrahim S, Keating M, Do KA, et al. CD38 expression as an important prognostic factor in B-cell chronic lymphocytic leukemia. *Blood*. 2001;98(1):181-186.
  36. Hamblin TJ, Davis Z, Gardiner A, Oscier DG, Stevenson FK. Unmutated Ig V(H) genes are associated with a more aggressive form of chronic lymphocytic leukemia. *Blood*. 1999;94(6):1848-1854.
  37. Krober A, Seiler T, Benner A, et al. V(H) mutation status, CD38 expression level, genomic aberrations, and survival in chronic lymphocytic leukemia. *Blood*. 2002;100(4):1410-1416.
  38. Polyak MJ, Li H, Shariat N, Deans JP. CD20 homo-oligomers physically associate with the B cell antigen receptor. Dissociation upon receptor engagement and recruitment of phosphoproteins and calmodulin-binding proteins. *J Biol Chem*. 2008;283(27):18545-18552.
  39. Ternynck T, Dighiero G, Follezu J, Binet JL. Comparison of normal and CLL lymphocyte surface Ig determinants using peroxidase-labeled antibodies. I. Detection and quantitation of light chain determinants. *Blood*. 1974;43(6):789-795.
  40. Jensen KD, Nori A, Tijerina M, Kopeckova P, Kopecek J. Cytoplasmic delivery and nuclear targeting of synthetic macromolecules. *J Control Release*. 2003;87(1-3):89-105.
  41. Hoster E, Dreyling M, Klapper W, et al. A new prognostic index (MIPI) for patients with advanced-stage mantle cell lymphoma. *Blood*. 2008;111(2):558-565.
  42. Robak T, Dmoszynska A, Solal-Celigny P, et al. Rituximab plus fludarabine and cyclophosphamide prolongs progression-free survival compared with fludarabine and cyclophosphamide alone in previously treated chronic lymphocytic leukemia. *J Clin Oncol*. 2010;28(10):1756-1765.
  43. Niederfellner G, Lammens A, Mundigl O, et al. Epitope characterization and crystal structure of GA101 provide insights into the molecular basis for type I/II distinction of CD20 antibodies. *Blood*. 2011;118(2):358-67.
  44. Camilleri-Broet S, Cassard L, Broet P, et al. Fc gamma RIIb is differentially expressed during B cell maturation and in B-cell lymphomas. *Br J Haematol*. 2004;124(1):55-62.